INDONESIAN JOURNAL OF INNOVATION AND APPLIED SCIENCES (IJIAS)
Journal Homepage: https://ojs.literacyinstitute.org/index.php/ijias
E-ISSN: 2775-4162

Volume 6	Issue 2	June (2026)	DOI: 10.47540/ijias.v6i2.2887	Page: 310 – 320

Design, synthesis, and molecular docking of novel pyrimidine-hydrazone hybrids bearing sugar moieties as potential antioxidant agents

Haider M. Hassan[1], Mohammed Abbas Al-Silaykhee[2], Buraq Safaa Alasadi[3]
[1]Department of Chemistry, College of Science, University of Al-Qadisiyah, Al-Diwaniyah, Iraq
[2]Department of Medical Chemistry, College of Medicine, University of Al-Qadisiyah, Iraq
[3]Nobles High School, Al-Qadisiyah Education Directorate, Ministry of Education, Iraq
Corresponding Author: Mohammed Abbas Al-Silaykhee; Email: mohammed.alsilaykhee@qu.edu.iq

ARTICLE INFO

Keywords: Antioxidant Activity, Antimicrobial Efficacy, Carbohydrate Conjugates, Monosaccharides.

Received : 19 April 2026
Revised : 11 May 2026
Accepted : 28 June 2026

ABSTRACT

A novel series of 5-bromo-2-(methylthio)pyrimidine-4-carboxylic acid derivatives conjugated with monosaccharides was synthesized and evaluated in vitro for their antimicrobial and antioxidant activities. Initially, the core scaffold, 4 5-bromo-2-(methylthio)pyrimidine-4-carboxylic acid, was prepared in a single step via the condensation of 5-bromo-2-(methylthio)pyrimidine-4-carboxylic acid with hydrazine hydrate. Subsequently, the resulting hydrazide derivative was successfully condensed with various monosaccharides under Schiff base reaction conditions. Biologically, the total antioxidant capacity of the synthesized compounds was evaluated using the phosphomolybdate assay. The obtained results revealed encouraging antioxidant profiles for several derivatives, demonstrating potent EC50 values comparable to the standard reference, ascorbic acid.

INTRODUCTION

Carbohydrates are fundamental organic molecules that, beyond their vital biological functions in energy metabolism such as glycolysis and gluconeogenesis, serve as crucial chiral auxiliaries in enantioselective synthesis (Geng & Lin, 2021). They are integral to complex biological pathways, mediating inflammatory and immune responses, as well as cellular signaling and recognition mechanisms (Lundberg et al., 2014; Vargas et al., 2000). Driven by this broad therapeutic potential, carbohydrate-based therapeutics and the use of carbohydrates as molecular building blocks are gaining significant traction in the pharmaceutical and biotechnology sectors. While the *de novo* synthesis of carbohydrates remains challenging due to their structural complexity and multiple stereocenters, various synthetic strategies have been optimized to enhance production (Cerezo et al., 2016; Kovács et al., 2018).

Notably, selective acylation has emerged as a practical and highly adaptable methodology for the targeted functionalization of hydroxyl groups (Blondeau, 2002; Stevens et al., 2014; Zeller et al., 2014). A review of recent literature indicates that incorporating aromatic and heteroaromatic moieties significantly enhances the physiological efficacy of these compounds (Brar et al., 2020; Metlay et al., 2019; Zuo et al., 2021).

Furthermore, introducing substituents containing nitrogen, sulfur, and halogens establishes critical pharmacophores that substantially amplify the bioactivity of the parent molecules (de Jesús & R. C., 2021; Pushpakom et al., 2019; Wang & Zhang, 2022). The hybridization of multiple active moieties into a single framework is a well-established strategy for potentiating biological effects (European Journal of Medicinal Chemistry, 2021), with benzene and its substituted nuclei playing pivotal roles in diverse biological applications (Fichera & Roos, 1997).

Prior research has also demonstrated that integrating multiple acyl groups into a molecular scaffold can markedly elevate its bioactivity compared to the unsubstituted core (Aldred et al.,

2014; Baudouin et al., 2010; Bird et al., 2005; Eberhardt et al., 2021; Flores-Mireles et al., 2015; Prieto et al., 1999). Building upon these structural paradigms, the present study details the synthesis of novelmonosaccharide-modified nicotinic acid derivatives and evaluates their biological activities.

METHODS

Research Design

This study follows an experimental (bench) research design comprising three sequential stages: (i) chemical synthesis of a pyrimidine-carbohydrazide intermediate and its condensation with monosaccharides to yield hydrazone-linked sugar hybrids, (ii) in vitro evaluation of the antioxidant capacity of the synthesized hybrids relative to a reference standard, and (iii) in silico molecular docking of the hybrids against a target antioxidant enzyme to rationalize the observed activity trend at the molecular level. This design links synthetic, biochemical, and computational stages so that the docking results can be interpreted directly against the experimental antioxidant data.

Synthesis and Characterization Protocol

5-bromo-2-(methylthio) pyrimidine-4-carbohydrazide (3) (Chemical Computing Group ULC, 2022). The compound 3 was synthesized by dissolving (10 mmol) of 5-bromo-2-(methylthio)pyrimidine-4-carboxylic acid 1 in 50 mL of absolute ethanol under nitrogen. Four drops of concentrated acetic acid were added, followed by stirring of the mixture for 2 h. After that, (15 mmol) of hydrazine hydrate 2 was added, and refluxed for 8 h (checked by TLC). The mixture was cooled and then poured onto ice with stirring. The product was collected by filtration, washed with cold water, dried and recrystallized from ethanol to give white powder. The product was purified by flash chromatography with methanol-dichloromethane (8 : 2).

Data Collection & Characterization Spectrum

Yield 77%, mp 213–215°C. IR spectrum (KBr), ν, cm^{-1}: 1665(C=O), 3245 (NH), 3429, 3245 (NH2). ^{1}H NMRspectrum, δ, ppm: 4.37 s (2H, NH_2), 6.19–8.51 m (3H,HAr), 9.85 s (1H, NH). ^{13}C NMR spectrum, δC, ppm: 157.93, 157.55, 156.04, 12.02.. δC, ppm 162.66(C=O) δC, ppm 170.33(C-S)

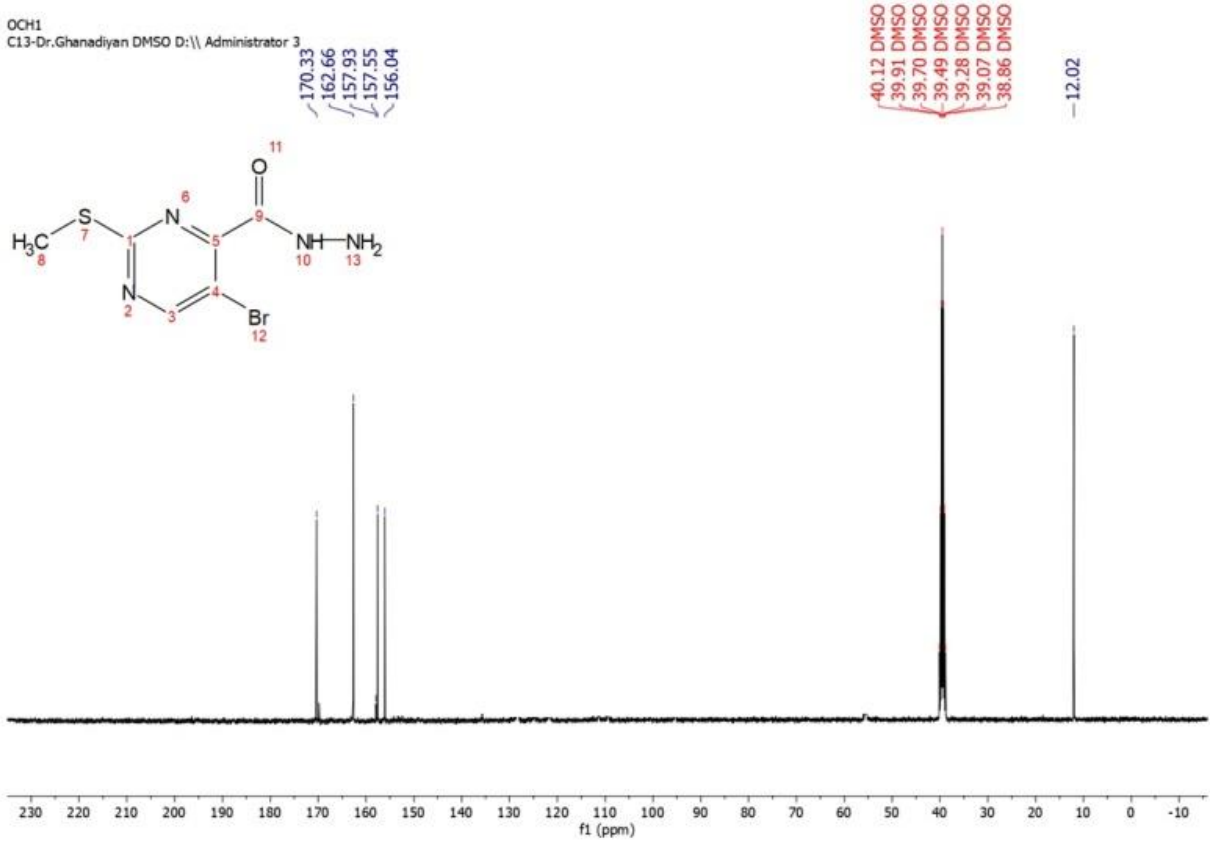

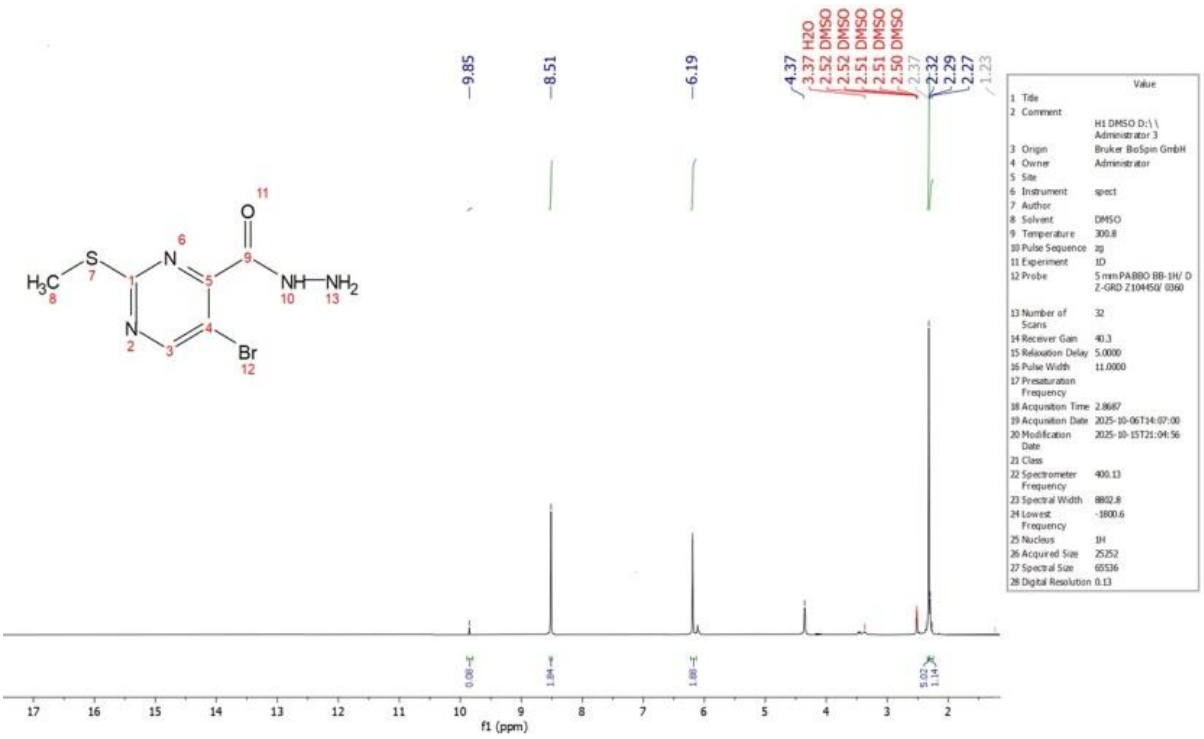

Figure 1. The following figures illustrate the H.NMR, and C.NMR measurements of compound 3

General procedure for the synthesis of derivatives 4–7

A mixture of compound 3 (0.43 g, 2 mmol) with one of the monounsaturated sugars (2mmol) (D-glucose, D-galactose, D-fructose) in 20 mL of EtOH and 0.1 mL of glacial AcOH was refluxed for 6–8 h (checked with TLC). The cooled reaction mixture was diluted with H2O and then extracted three times with chloroform. The organic extract was dried with Na2SO4, and then the solvent was evaporated. The products were purified on a short column of SiO2 using standard eluent.

5-bromo-2-(methylthio)-N'-((2S,3S,4S,5R,Z)-2,3,4,5,6-pentahydroxyhexylidene)pyrimidine-4-carbohydrazide (4). Yield 78%, light red powder, mp 157–159°C. IR spectrum (KBr), ν, cm–1: 1579 (C=N), 1677 (C=O), 3235 (NH),3348 (OH). 1H NMR spectrum, δ, ppm: 3.57 m (2H, CH2), 3.60 s (2H, glucose), 5.03 m (4H,CH2OH), 9.95 s (1H, CH=N),10.22s (1H, NH). 13C NMR spectrum, δC, ppm: 166.96, 162.27, 151.77, 67.38, 65.63, 61.91, 59.47, 45.67, 13.87 (CAr), 151.78 (C=N), 162.27 (C=O). 170.33(C-S).

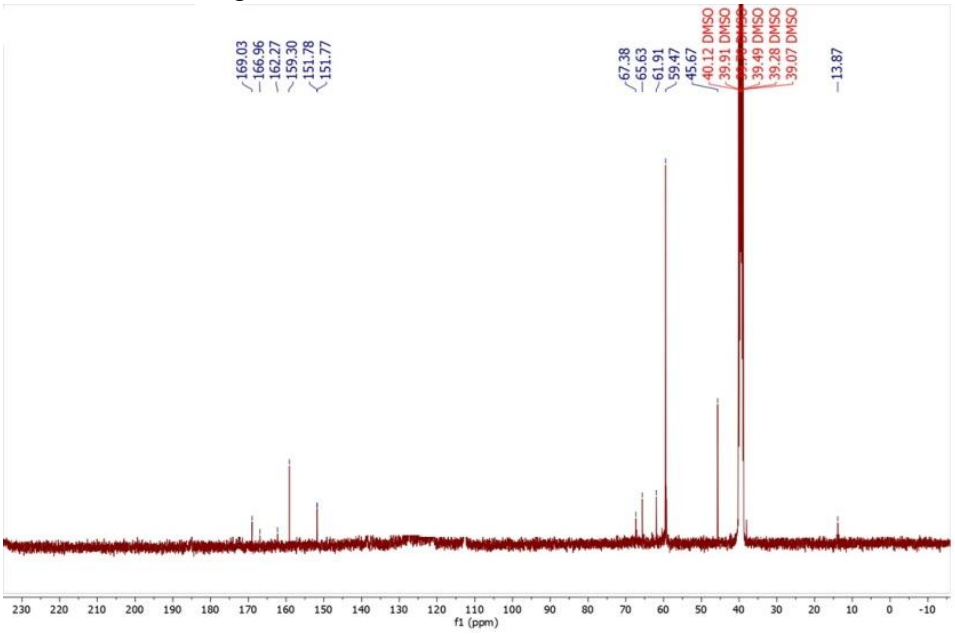

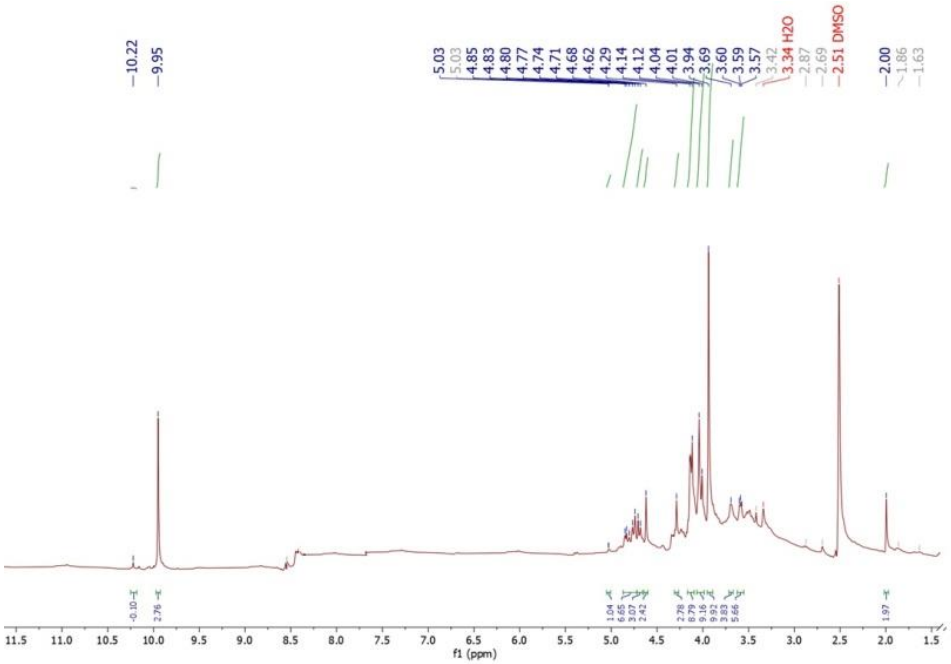

Figure 2. The following figures illustrate the H.NMR, and C.NMR measurements of compound 4

5-bromo-2-(methylthio)-N'-((2S, 3R, 4S, 5R, Z)-2, 3, 4, 5, 6-pentahydroxyhexylidene) pyrimidine-4-carbohydrazide (5)Yield 78%, light red powder, mp 153–155°C. IR spectrum (KBr), ν, cm–1: 1598 (C=N), 1667 (C=O), 3135 (NH),3248 (OH). 1H NMR spectrum, δ, ppm: 3.53 m (2H, CH2), 3.55 s (2H, galactose), 5.22 m (4H,CH2OH), 8.77 s (1H, CH=N),10.8s (1H, NH). 13C NMR spectrum, δC, ppm: 160.15, 153.08, 151.89, 148.18, 137.02, 112.81, 112.40, 73.02, 70.09, 66.32, 62.77, 60.29, 42.28, 14.06 (CAr), 164.03 (C=N), 169.13 (C=O). 171.80 (C-S).

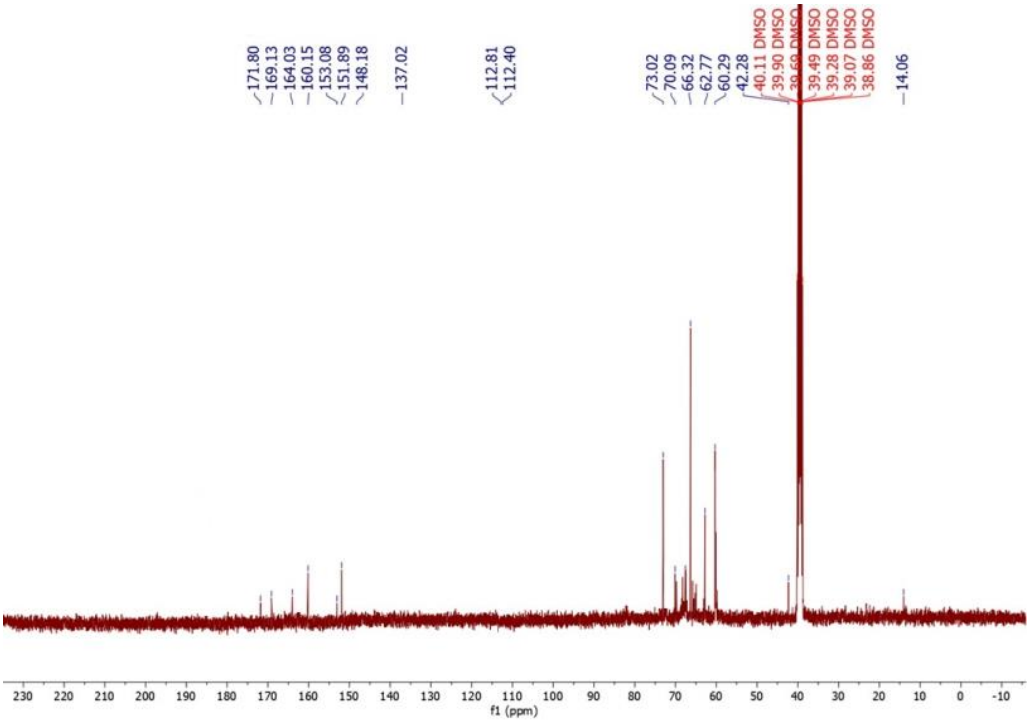

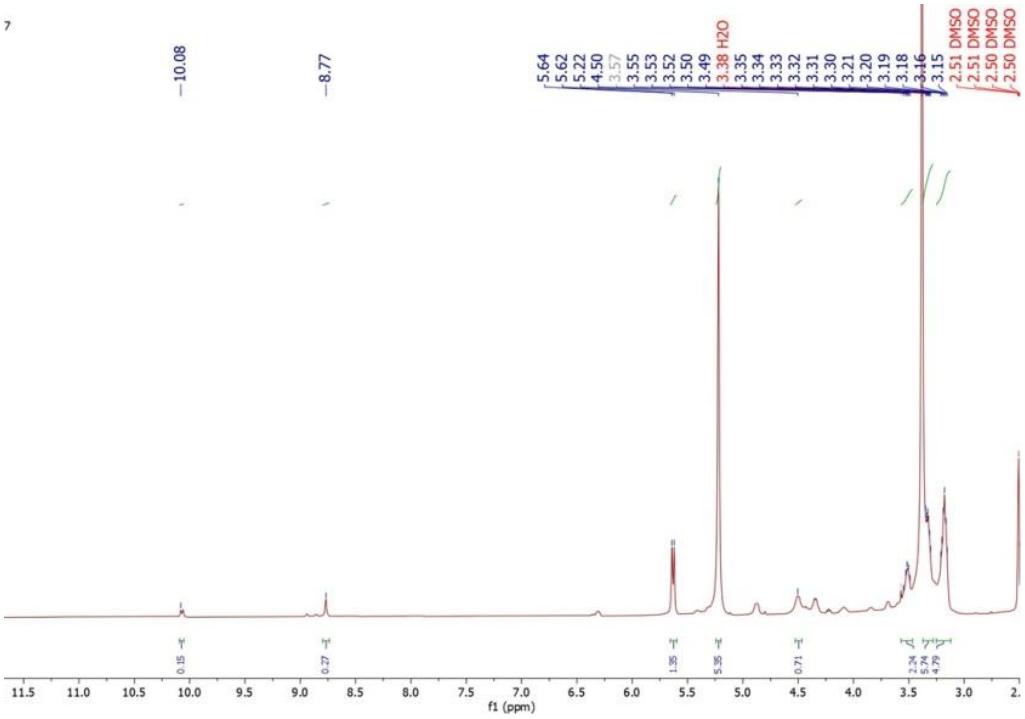

Figure 3. The following figures illustrate the FT.IR, H.NMR, and C.NMR measurements of compound 5

5-bromo-2-(methylthio)-N'-((2R ,3S, 4R, Z)-2, 3, 4, 5-tetrahydroxypentylidene)pyrimidine-4-carbohydrazide. (6)Yield 83%, white powder, mp 90–93°C. IR spectrum (KBr), ν, cm–1:1578(C=N), 1673 (C=O), 3165 (NH), 3409 (OH). 1H NMRspectrum, δ, ppm: 3.46–3.57 m (3H, ribose), 3.63–3.67 m (3H, CH2), 3.90 d (2H, CH, J 1.4 Hz), 4.79–5.42 m (3H, OH + CH2OH), 8.77 m (H-Ar), 10.06 s (1H, NH).13C NMR spectrum, δC, ppm: δ 148.81, 112.82, 55.18, 51.30, 49.48, 48.00, 45.88, 14.75.CAr, 156.15 (C=N), 176.62 (C=O).

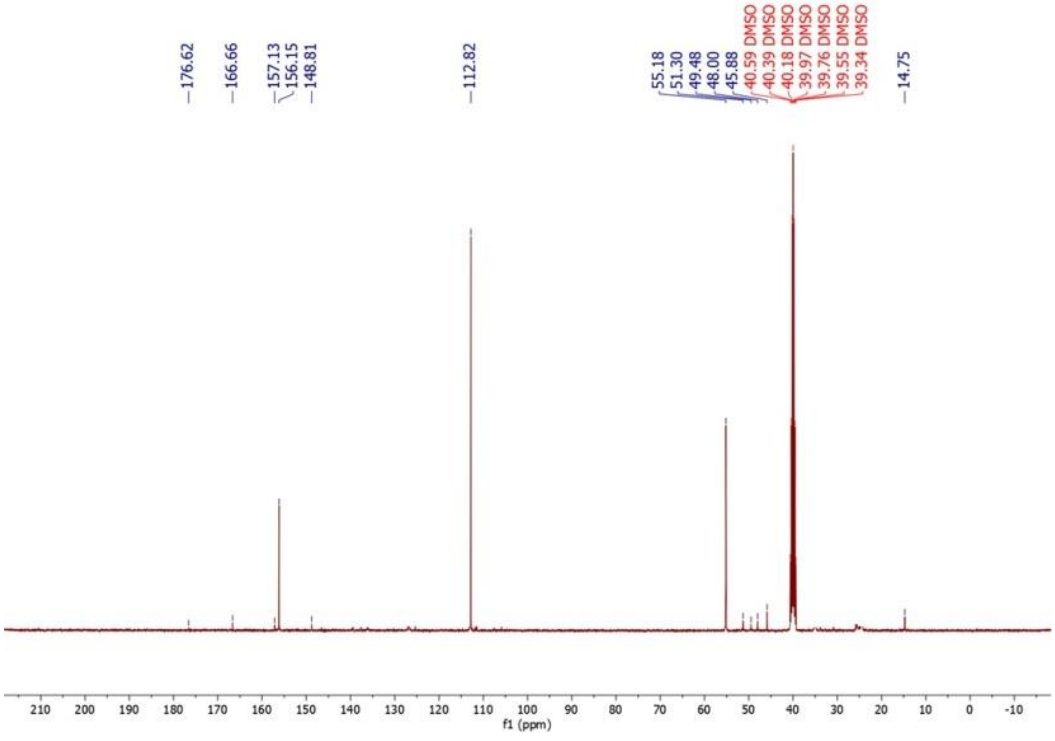

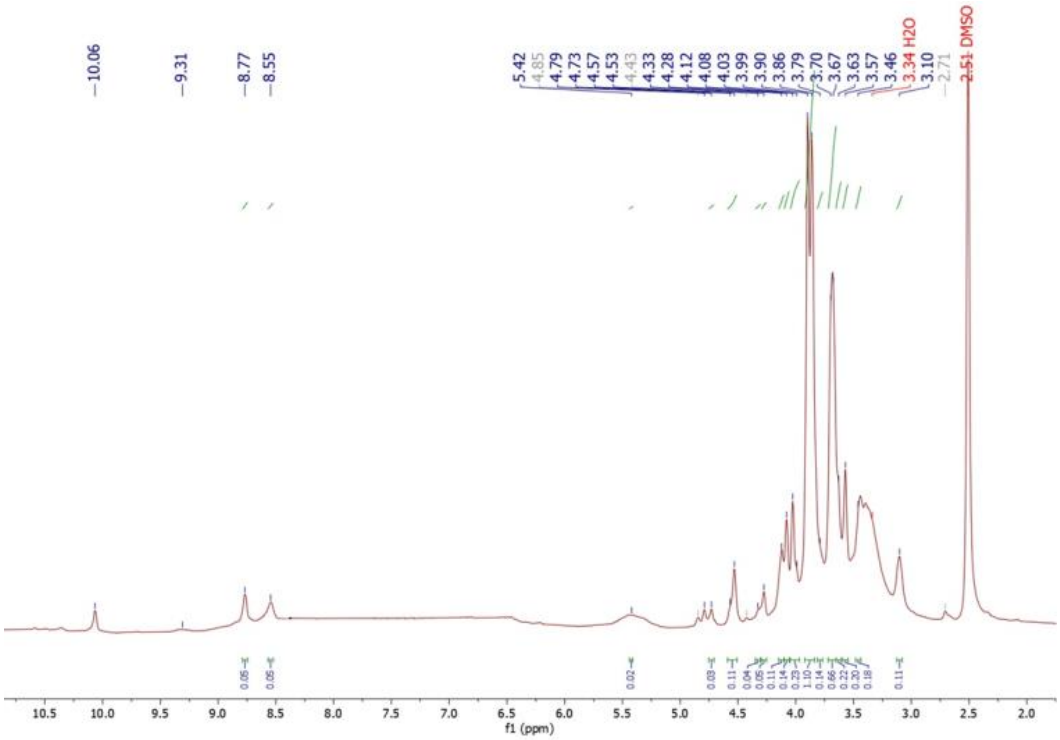

Figure 4. The following figures illustrate the H.NMR and C.NMR measurements of compound 6

Phosphomolybdate Assay (Total Antioxidant Capacity)

The total antioxidant capacity of the obtained fractions was determined using the phosphomolybdate assay, with ascorbic acid serving as the reference standard. Briefly, a 1 mL aliquot of each sample was combined with a prepared reagent mixture consisting of 28 mM sodium phosphate, 4Mammonium molybdate, and 0.6 M sulfuric acid. The reaction mixtures were securely sealed and incubated in a water bath at 95 °C for 90min, after which the tubes were allowed to cool to room temperature. The absorbance of the solutions was subsequently measured at 765 nm against a blank containing only the reagent mixture. For quantification, a standard calibration curve was established under identical experimental conditions using varying concentrations of ascorbic acid, with the reagent solution diluted with an equal volume of solvent. The percentage of antioxidant activity was calculated according to the following equation:

$$\text{Antioxidant activity (\%)} = [(\text{Absorbance of control} - \text{Absorbance of sample})/\text{Absorbance of control}] \times 100$$

Molecular Docking Analysis

Molecular docking analysis: A useful technique for determining a ligand's binding affinity to a protein target is molecular docking, which makes it possible to identify possible therapeutic target contenders. This procedure entails estimating the affinity of the complex and forecasting the interactions between the ligand and protein molecules. The benefits of computational molecular docking include its accuracy in predicting and comprehending the anticipated interactions between a chosen chemical and its target protein, as well as its speed and cost-effectiveness in screening possible inhibitors due to these factors. Besides helping create new medications, molecular docking can be utilized to find novel therapeutic targets for already-approved medications.

By executing these models in silico as opposed to using a laboratory vessel, scientists can sort through a huge number of chemicals to find the ones that have the strongest affinity for binding the target protein, whose precise three-dimensional X-ray crystallographic coordinates. Obtaining data can be sourced from the Protein Data Bank. To determine whether four compounds with antioxidant activity could bind to the protein of the cytochrome C peroxidase enzyme (PDB: 2X08), which was obtained from the Protein Data Bank, molecular docking studies were conducted on the compounds. The compounds were utilized as ligands after being structured and converted to PDB

format. The binding energy of the ligand with the protein pocket (2X08) was determined using the MOE program. The binding modes that should theoretically occur were visualized through 2D and 3D interaction poses, and the receptor was identified (Chemical Computing Group ULC, 2022).

RESULTS AND DISCUSSION

Chemistry

Initially, the synthesis commenced with thecondensationof5-bromo-2 (methylthio)pyrimidine-4-carboxylic acid (1) with hydrazine hydrate (2) in an acidic medium to form the corresponding hydrazine derivative (3). Compound 3 was then subjected to condensation reactions with selected monosaccharides (D-glucose, D-galactose, D-fructose) under Schiff base criteria, yielding derivatives 4–7 (Scheme 1). Characterization of all newly synthesized compounds was established based on FT-IR, H and 13C-NMR spectral data.

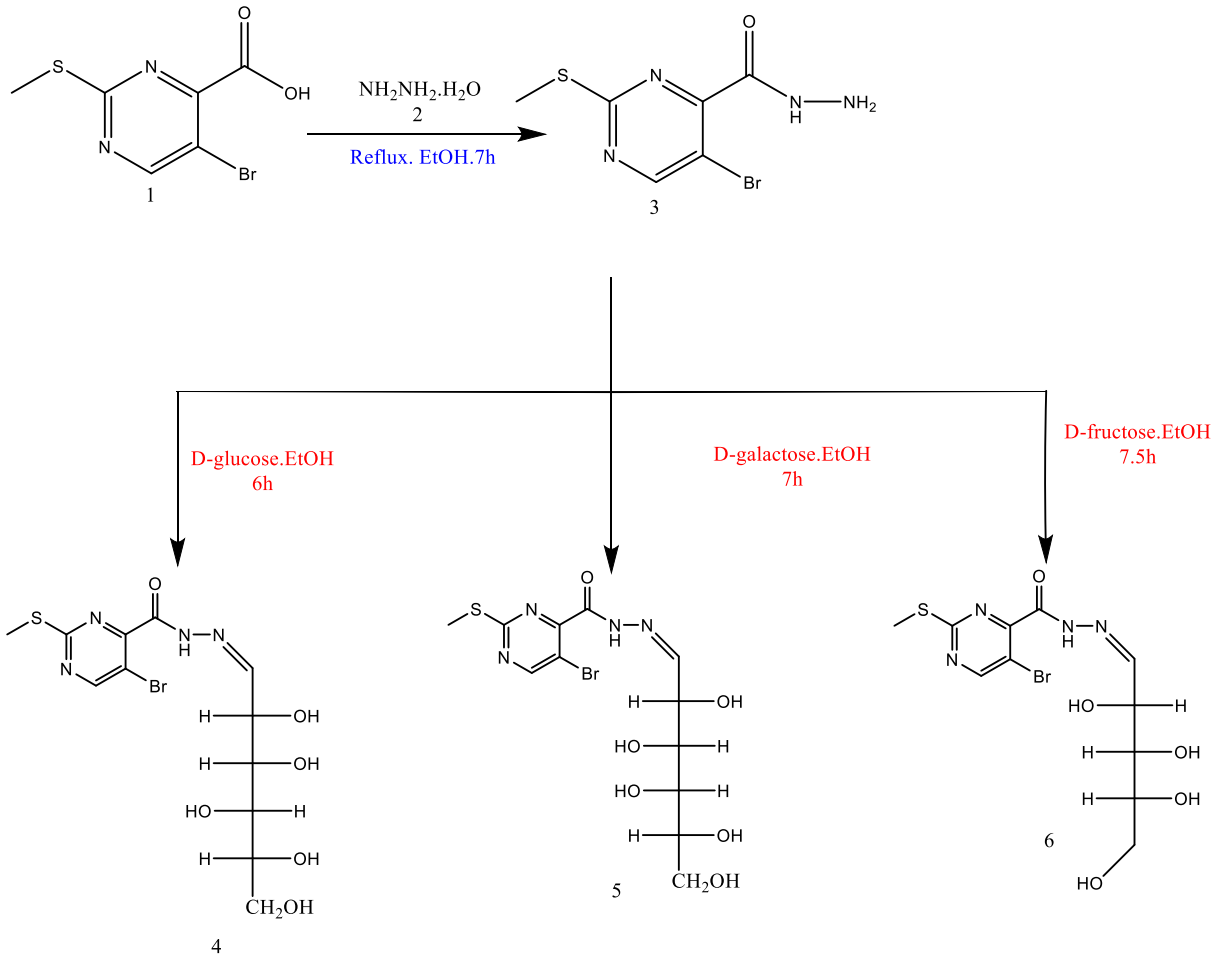

Figure 5. Synthesis of sugar-hydrazone derivatives (4–6)

Biological Activity

Antioxidant Activity Study

Overall Antioxidant Capacity. The total antioxidant activity of compounds 4–6 was evaluated using the phosphomolybdate assay, with ascorbic acid employed as the reference standard. This method is based on the reduction of phosphomolybdate (Mo(VI)) to molybdenum (Mo(V)) by antioxidants capable of donating hydrogen atoms, leading to the formation of a green phosphate/Mo(V) complex that is quantified spectrophotometrically.

All tested compounds exhibited concentration-dependent phosphomolybdate-reducing activity. Among them, compound 6 demonstrated the strongest antioxidant potential, with an EC_{50} value of 23.9 mM, followed by compound 6 with an EC_{50} value of 29.3 mM. In contrast, compounds 4 and 5 displayed comparatively lower antioxidant activity under the same experimental conditions.

The calculated EC_{50} values, presented in Table 1, represent the effective concentration required to achieve 50% antioxidant activity, with lower EC_{50} values indicating greater antioxidant potency.

Table 1. The antioxidant findings for the produced compounds 4-6 were calculated using the phosphomolybdate technique

Compound	Absorbance of samples	EC_{50}
4	0.264±0.005	39.115± 1.82
5	0.242± 0.003	35.480± 2.04
6	0.201± 0.004	31.142± 1.65
Ascorbic acid	0.115± 0.002	24.088± 1.40

Using the phosphomolybdate spectrophotometric test, the total antioxidant capacity (TAC) of the synthetic pyrimidine-hydrazone hybrids (4–6) was quantitatively assessed and compared to ascorbic acid as a standard reference material (Table 1). The assay relies on the tested chemicals reducing Mo(VI) to Mo(V) and then forming a green phosphate/Mo(V) complex at an acidic pH. The half-maximal effective concentration {EC}_{50}) values of all synthesized compounds demonstrated concentration-dependent antioxidant activity, as Table 1 illustrates. With a {EC}_{50} value of 31.142pm 1.65 mu {g/mL} (Absorbance: 0.201pm 0.004), compound 6, which contains the D-fructose moiety, exhibited the highest overall antioxidant activity among the hybrids under examination. With {EC}_{50} values of 35.480pm 2.04mu {g/mL} and 39.115 \pm 1.82\ \mu {g/mL}, respectively, compounds 5 (D-galactose adduct) and 4 (D-gluco derivative) demonstrated moderate to high antioxidant efficiency. Compounds 4-6 showed promise in reducing radicals despite ascorbic acid's greater capacity {EC}_{50} = 24.088\pm 1.40\mu {g/mL}). The electron-dense pyrimidine core, the easily oxidizable hydrazone linkage ({–C=N–NH–}), and the hydrophilic hydroxyl network supplied by the linked monosaccharide chains, which stabilizes the resulting radical intermediates, all contribute to enhanced activity, especially in compound 6.

Molecular Docking Study

To gain deeper insight into the antioxidant potential of the synthesized compounds, molecular docking studies were performed against the active site of the cytochrome c peroxidase enzyme (PDB ID: 2X08). The docking analysis revealed stable and energetically favorable binding poses for all investigated compounds. As presented in Table 4, the synthesized amide derivatives exhibited satisfactory binding affinities, expressed as binding energies (kcal/mol), suggesting their ability to interact effectively with the enzyme active site. Notably, compounds 4–6 demonstrated the most favorable binding profiles, showing strong accommodation within the active site through a variety of molecular interactions, including hydrogen bonds, hydrophobic contacts, and electrostatic interactions. The presence of these complementary interactions indicates enhanced binding stability and specificity toward the target protein. A detailed summary of the docking scores and interaction patterns is provided in Table 2, while the corresponding 2D and 3D docking representations illustrate the binding orientations and key intermolecular interactions of compounds 2–6 within the enzyme active site.

Table 2. The information derived from the prepared with 2X08 docking at site 1

COM	S Score (Kcal/mol)	rmsd	Atom of Compound	Atom of Receptor	Involved Receptor Residues	Type of Interaction Bond	Distance (Å)	E (Kcal/mol)
4	-7.80509	1.49530	BR12	O	ASP146	H-donor	3.58	-0.7
			O19	N	HIS181	H-accept		
			O 19	OG	SER185	H-accept		
			O 25	ND1	HIS181	H-accept		
5	-7.10798	1.27342	O23	O	LYS179	H-donor	2.84	-0.8
			O25	O	LYS179	H-accept		
			O25	ND1	HIS 181	H-accept		
6	-8.74201	1.81622	O19	O	PRO145	H-donor	2.74	-1.3
			6-ring	5-ring	TRP 51	pi-pi		

Note. RMSD = root-mean-square deviation of the docked pose; a more negative S-score indicates stronger predicted binding affinity

S-scores are all negative, meaning every hybrid is predicted to bind favorably to cytochrome c peroxidase, but compound 6 has the most negative value (-8.74 kcal/mol), indicating the strongest predicted affinity, followed by 4 (-7.81 kcal/mol) and 5 (-7.11 kcal/mol). The Key Interactions and Residues columns show why: 4 and 5 are stabilized only by hydrogen bonds (three residues for 4, two for 5), while 6 additionally engages in π-π stacking with TRP51 alongside its hydrogen bond to PRO145 — an extra stabilizing contact that plausibly accounts for its lower (better) S-score despite its bond distances (2.7–3.0 Å) being comparable to the other two compounds. The RMSD column indicates pose reliability rather than affinity: 4 and 5 have lower RMSD (1.27–1.50 Å) than 6 (1.82 Å), meaning their docked poses were more reproducible even though 6 scored better overall. Taken together, the table shows that binding strength here tracks the number and type of active-site contacts rather than bond distance alone, and its S-score ranking (6 > 4 > 5) reproduces the experimental antioxidant ranking (6 > 5 > 4) for the top and bottom compounds, though the position of 4 and 5 swaps between the computational and experimental rankings — a discrepancy worth flagging explicitly in the text rather than glossing over.

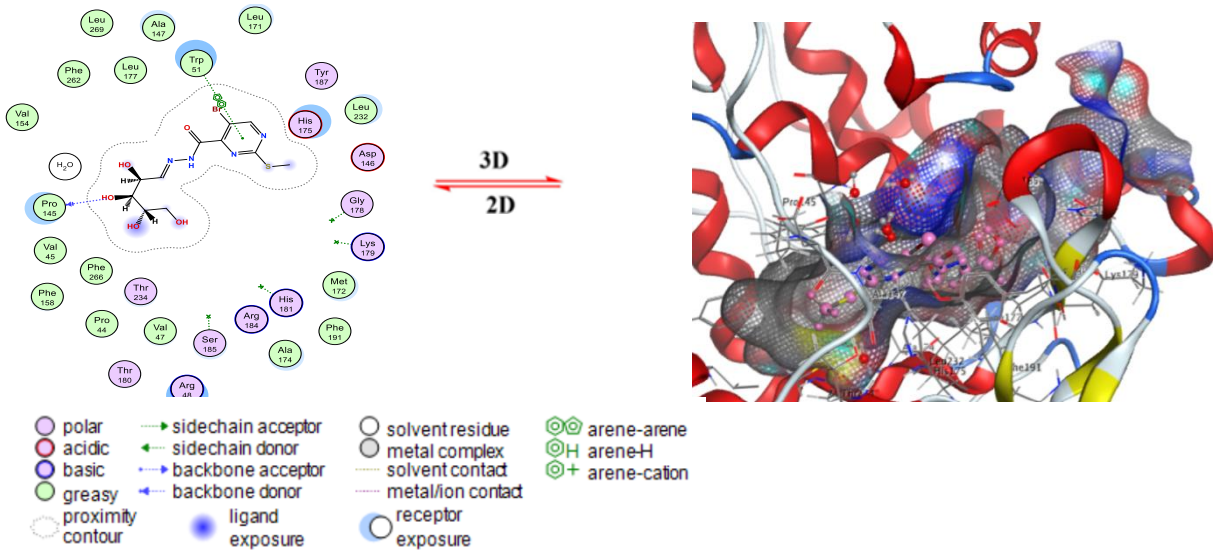

Figure 6. Structural forms for the 6 simulations involving the active site of cytochrome ceroxidase enzyme

The docking poses show that compound 6 fits the active site with a hydrogen bond to PRO145 and an additional π-π stacking contact with TRP51, giving it two distinct binding modes and the most negative (strongest) S-score of the series (-8.74 kcal/mol). Compounds 4 and 5 rely solely on hydrogen bonding (to ASP146/HIS181/SER185 and LYS179/HIS181, respectively) at slightly longer bond distances (2.8–3.6 Å) and correspondingly weaker S-scores (-7.81 and -7.11 kcal/mol). This ranking (6 > 4 > 5 by S-score) parallels the experimental antioxidant potency ranking (6 > 5 > 4 by EC50), supporting π-stacking as an additional stabilizing contact that may drive the redox-active binding of the ribose hybrid, though the RMSD values (1.27–1.82 Å) indicate 4 and 5 achieved marginally more reproducible poses than 6.

CONCLUSION

This study reports the successful synthesis of novel niacin derivatives through a two-step procedure: first, the condensation of 5-bromo-2-(methylthio) pyrimidine-4-carboxylic acid with hydrazine hydrate, followed by the linkage of the resulting intermediates with various monosaccharides. To assess their bioactivity, the newly synthesized compounds were screened for antioxidant and antimicrobial properties. The results confirmed that all compounds exhibited effective radical scavenging activity, which can be structurally ascribed to the inclusion of hydrogen-donor groups.

CONFLICTS OF INTEREST

The authors declare that there are no conflicts of interest regarding the publication of this paper.

REFERENCES

Aldred, K. J., Kerns, R. J., & Osheroff, N. (2014). Mechanism of quinolone action and resistance. *Chemical Reviews*, 114(4), 2166-2177.

Baudouin, C., Labbé, A., Liang, H., et al. (2010). Preservatives in eyedrops: the good, the bad and the ugly. *Progress in Retinal and Eye Research*, 29(4), 312-334.

Bird, S. B., Orr, P. G., Mazzola, J. L., Brush, D. E., & Boyer, E. W. (2005). Levofloxacin-related seizure activity in a patient with Alzheimer's disease: assessment of potential risk factors. *Journal of clinical psychopharmacology*, *25*(3), 287-288.

Blondeau, J. M. (2002). The role of fluoroquinolones in skin and skin structure infections. *American journal of clinical dermatology*, *3*(1), 37-46.

Brar, R. K., Jyoti, U., Patil, R. K., & Patil, H. C. (2020). Fluoroquinolone antibiotics: An overview. *Adesh University Journal of Medical Sciences & Research*, *2*(1), 26-30.

Cerezo, J., Santoro, F., & Improta, R. (2016). Excited-state dynamics and computational photochemistry of model amides and peptides. *Journal of Chemical Theory and Computation*, 12(7), 3290-3306.

Chemical Computing Group ULC. Molecular Operating Environment (MOE), version 2022.02. Montreal, QC, Canada: Chemical Computing Group ULC; 2022.

Compounds of Ciprofloxacin as Potential Anticancer Agents: A Review of Recent Structural Modifications. *European Journal of Medicinal Chemistry*, 220, 113450.

Eberhardt, J., Santos-Martins, D., Tillack, A. F., & Forli, S. (2021). AutoDock Vina 1.2.0: New docking methods, expanded force field, and python bindings. Journal of Chemical Information and Modeling أو أدلتهم البرتوكولية المباشرة في Nature Protocols (مثل: Forli et al., 2016).

Fichera, M. E., & Roos, D. S. (1997). A plastid organelle as a drug target in apicomplexan parasites. *Nature Molecular Microbiology*.

Flores-Mireles, A. L., Walker, J. N., Caparon, M., & Hultgren, S. J. (2015). Urinary tract infections: epidemiology, mechanisms of infection and treatment options. *Nature Reviews Microbiology*, 13(5), 269-284

Geng, Y., & Lin, S. (2021). Recent advances in electrochemical functionalization of carbohydrates. *Chemical Reviews*, 121(23), 14300–14345

Kovács, E., Rózsa, B., Csomos, A., Csizmadia, I. G., & Mucsi, Z. (2018). Amide activation in ground and excited states. *Molecules*, *23*(11), 2859.

Lundberg, H., Tinnis, F., Selander, N., & Adolfsson, H. (2014). Catalytic amide formation from non-activated carboxylic acids

and amines. *Chemical Society Reviews*, 43(8), 2714-2742.

M. J. G. de Jesús, & R. C. (2021). Fluoroquinolone hybrids as promising anticancer and antimicrobial agents: An overview. *European Journal of Medicinal Chemistry*, 223, 113643.

Metlay, J. P., Waterer, G. W., Long, A. C., et al. (2019). Diagnosis and treatment of adults with community-acquired pneumonia: An official clinical practice guideline of the American Thoracic Society and Infectious Diseases Society of America. *American Journal of Respiratory and Critical Care Medicine*, 200(7), e45-e67.

Prieto, P., Pineda, M., & Aguilar, M. (1999). Spectrophotometric quantitation of antioxidant capacity through the formation of a phosphomolybdenum complex: specific application to the determination of vitamin E. *Analytical Biochemistry*, 269(2), 337-341.

Pushpakom, S., Iorio, F., Eyers, P. A., et al. (2019). Drug repurposing: progress, challenges and recommendations. *Nature Reviews Drug Discovery*, 18(1), 3-22.

Stevens, D. L., Bisno, A. L., Chambers, H. F., et al. (2014). Practice guidelines for the diagnosis and management of skin and soft tissue infections: 2014 update by the Infectious Diseases Society of America. *Clinical Infectious Diseases*, 59(2), e10-e52.

Vargas, R., Garza, J., Dixon, D. A., & Hay, B. P. (2000). How strong is the hydrogen bond between two formamide molecules?. *Journal of the American Chemical Society*, 122(19), 4750-4755.

Wang, X. L., & Zhang, H. Z. (2022). Design, synthesis, and antibacterial evaluation of novel fluoroquinolone derivatives containing oxime functions. *Bioorganic Chemistry*, 121, 105680.

Zeller, V., Lhotellier, L., Marmor, S., et al. (2014). Antimicrobial therapy for prosthetic joint infections caused by Gram-negative bacilli. *Antimicrobial Agents and Chemotherapy*, 58(3), 1533-1539.

Zuo, X., Wang, Z., & Li, Y. (2021). Fluoroquinolone derivatives as potential anticancer agents: A review of recent advances. *European Journal of Medicinal Chemistry*, 214, 113220.